

**ESR studies of organic conductors with  
bis(ethylenedithio)tetrathiafulvalene (BEDT-TTF), (BEDT-TTF)<sub>2</sub>ClO<sub>4</sub>(C<sub>2</sub>H<sub>3</sub>Cl<sub>3</sub>)<sub>0.5</sub>,  
and (BEDT-TTF)<sub>3</sub>(ClO<sub>4</sub>)<sub>2</sub>, and their two-dimensionality**

Toshiaki Enoki, Kenichi Imaeda, Mototada Kobayashi, and Hiroo Inokuchi  
*Institute for Molecular Science, Myodaiji, Okazaki 444, Japan*

Gunzi Saito  
*Institute for Solid State Physics, University of Tokyo, Minato-ku, Tokyo 106, Japan*

(Received 17 June 1985)

The magnetic properties of two (BEDT-TTF)-ClO<sub>4</sub> radical salts, (BEDT-TTF)<sub>2</sub>ClO<sub>4</sub>(C<sub>2</sub>H<sub>3</sub>Cl<sub>3</sub>)<sub>0.5</sub> and (BEDT-TTF)<sub>3</sub>(ClO<sub>4</sub>)<sub>2</sub>, have been investigated by means of ESR measurements. For the former (2:1:0.5)-phase crystal, the susceptibility shows a nesting transition at 20 K, which is affected by the degree of the incompleteness in the ordering of the C<sub>2</sub>H<sub>3</sub>Cl<sub>3</sub> molecules below 200 K. The large linewidth suggests two-dimensionality, consistent with the low *T<sub>c</sub>* of the nesting instability and the small anisotropy in the resistivity in the *a-c* plane. In the case of the latter (3:2)-phase crystal, the susceptibility shows a metal-insulator transition at 150 K. Below *T<sub>c</sub>*, an insulating state with a spin singlet is stabilized after the displacement of the BEDT-TTF [(C<sub>5</sub>H<sub>4</sub>S<sub>4</sub>)<sub>2</sub>] molecules in a one-dimensional chain through the Peierls instability. The large linewidth also suggests two-dimensionality.

## I. INTRODUCTION

Organic conductors have metal-insulator transitions inevitably for their low dimensionality. To suppress metal-insulator transitions and to design organic superconductors, many efforts have been made with chemical modifications of a TTF [C<sub>6</sub>H<sub>4</sub>S<sub>4</sub>, with the structural formula 2,2'-bi(1,3-dithole-2-ylidene)] molecule. Important requirements for such low-temperature organic metals are to decrease on-site Coulomb repulsion and to increase dimensionality. Substitution of S atoms in a TTF moiety with Se atoms has led to superconductivity in (TMTSF)<sub>2</sub>ClO<sub>4</sub>,<sup>1</sup> and several interesting organic metals were obtained by means of substitution with Te atoms.<sup>2,3</sup>

We have presented a low-temperature organic metal with a donor BEDT-TTF [bis(ethylenedithio)tetrathiafulvalene or (C<sub>5</sub>H<sub>4</sub>S<sub>4</sub>)<sub>2</sub>] which is obtained with the introduction of substitutional groups of a six-membered ring with S atoms to a TTF moiety. The donor molecule BEDT-TTF forms radical cation salts (BEDT-TTF)-*X*, where *X* is an inorganic anion such as ClO<sub>4</sub><sup>-</sup>, ReO<sub>4</sub><sup>-</sup>, BrO<sub>4</sub><sup>-</sup>, IO<sub>4</sub><sup>-</sup>, PF<sub>6</sub><sup>-</sup>, AsF<sub>6</sub><sup>-</sup>, SbF<sub>6</sub><sup>-</sup>, or I<sub>3</sub><sup>-</sup>. Unlike (TMTTF)<sub>2</sub>*X* (Refs. 4 and 5) and (TMTSF)<sub>2</sub>*X* (Ref. 1), BEDT-TTF complexes show a multiplicity of stoichiometries, crystal structures, and inclusion of solvent molecules, because a BEDT-TTF molecule has a nonplanar structure affected by the thermal motions of

the ethylene groups as seen in the molecular structure shown in Fig. 1.

For (BEDT-TTF)-ClO<sub>4</sub> complexes, two phases are obtained through electrocrystallization with trichloroethane solvent. (BEDT-TTF)<sub>2</sub>ClO<sub>4</sub>(C<sub>2</sub>H<sub>3</sub>Cl<sub>3</sub>)<sub>0.5</sub> indicates two-dimensional metallic conductivity down to 1.4 K.<sup>6</sup> BEDT-TTF molecules have a side-by-side arrangement to form a one-dimensional chain, where the intermolecular S-S contacts are considerably shorter than the van der Waals distance (3.7 Å).<sup>7-10</sup> The cooperation of the side-by-side and the face-to-face intermolecular interactions gives the two-dimensional characters in the electronic properties. (BEDT-TTF)<sub>3</sub>(ClO<sub>4</sub>)<sub>2</sub> shows a sharp metal-insulator transition at 174 K as a quasi-one-dimensional system.<sup>9</sup>

Recently, superconductivity of (BEDT-TTF)<sub>2</sub>ReO<sub>4</sub> was observed near 2 K under pressures above 4 kbar, as the first observation among sulfur-donor organic conductors.<sup>11</sup> Moreover, (BEDT-TTF)<sub>2</sub>I<sub>3</sub> was found to have a superconducting transition at 1.5 K under ambient pressure<sup>12,13</sup> and at 8 K under a high pressure.<sup>14,15</sup>

We are interested in the effects of polymorphism and the introduced solvent on the electronic properties of a two-dimensional metal (BEDT-TTF)<sub>2</sub>ClO<sub>4</sub>(C<sub>2</sub>H<sub>3</sub>Cl<sub>3</sub>)<sub>0.5</sub> and a quasi-one-dimensional metal (BEDT-TTF)<sub>3</sub>(ClO<sub>4</sub>)<sub>2</sub>. In this paper, the ESR results are presented for these two compounds, in order to clarify the correlation between their electronic properties and crystal structures.

## II. EXPERIMENTAL RESULTS

The single crystals of (BEDT-TTF)<sub>3</sub>(ClO<sub>4</sub>)<sub>2</sub> and (BEDT-TTF)<sub>2</sub>ClO<sub>4</sub>(C<sub>2</sub>H<sub>3</sub>Cl<sub>3</sub>)<sub>0.5</sub> were prepared using a standard electrochemical technique. A 2 × 10<sup>-4</sup>M solu-

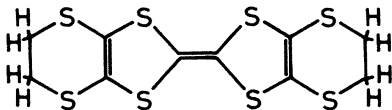


FIG. 1. The molecular structure of BEDT-TTF.

tion of BEDT-TTF in 100 ml of purified  $C_2H_3Cl_3$  was reacted with  $(1.5-3.0) \times 10^{-3} M$   $(C_4H_9)_4NClO_4$  under a constant current (5 and 10  $\mu A$ ) for a week. Two kinds of black crystals were simultaneously obtained as thin plates and thicker plates. The former was recognized as  $(BEDT-TTF)_3(ClO_4)_2$  [(3:2) phase] and the latter as  $(BEDT-TTF)_2ClO_4(C_2H_3Cl_3)_{0.5}$  [(2:1:0.5) phase] by means of x-ray diffraction. The crystal data were as follows: (2:1:0.5) phase, triclinic,  $a = 13.1$  Å,  $b = 17.7$  Å,  $c = 7.8$  Å,  $\alpha = 79.3^\circ$ ,  $\beta = 104.7^\circ$ ,  $\gamma = 110.9^\circ$ ,  $V = 1690$  Å<sup>3</sup>,  $Z = 2$ ; (3:2) phase, triclinic,  $a = 16.4$  Å,  $b = 9.5$  Å,  $c = 7.6$  Å,  $\alpha = 95.9^\circ$ ,  $\beta = 87.2^\circ$ ,  $\gamma = 90.8^\circ$ ,  $V = 1182$  Å<sup>3</sup>,  $Z = 1$ . It was found that the (2:1:0.5) phase was mainly obtained under a low applied current (5  $\mu A$ ), while the (3:2) phase under a higher one (10  $\mu A$ ). The typical dimensions of the crystals were  $1 \times 1 \times 0.2$  and  $2 \times 1.5 \times 0.01$  mm<sup>3</sup> for the (2:1:0.5) phase and the (3:2) phase, respectively.

The ESR spectra were measured between liquid-helium and room temperatures with a conventional Varian Associates X-band E112 spectrometer equipped with a data acquisition system. The temperature control was achieved using an Oxford Instruments ESR9 continuous-flow helium cryostat. The samples were mounted on a Teflon holder in a 4-mm-diam quartz ESR tube with 20-Torr He exchange gas. The accuracy of the sample setting was within 5°. The microwave power supplied into a cavity was below 1 mW to avoid a saturation effect of the ESR spectra. The absolute magnitude of the spin susceptibility was determined with diphenylpicrylhydrazyl as a reference.<sup>16</sup> A peak-to-peak linewidth was adopted for a linewidth.

Figure 2 shows the temperature dependence of the ESR intensity of the (2:1:0.5) phase for a heating run just after a rapid cooling of the sample (cooling rate: 40 K/h). The intensity is almost constant in the high-temperature region down to about 200 K, while it decreases gradually until about 80 K. At low temperatures it has a Curie tail, where the concentration of localized spins is about 0.1–0.3% of the BEDT-TTF molecules. The intensity for slow cooling (cooling rate: 5 K/h) exhibits a different temperature dependence from that for rapid cooling, as shown in Fig. 3. The intensity shows an abrupt decrease at about 20 K, though it has the similar temperature

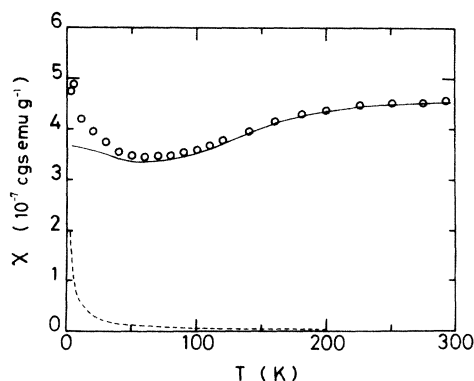


FIG. 2. Temperature dependence of the ESR intensity of the (2:1:0.5) phase for rapid cooling. The solid line is obtained after the subtraction of the Curie tail at low temperatures. The Curie susceptibility is shown by the dashed line.

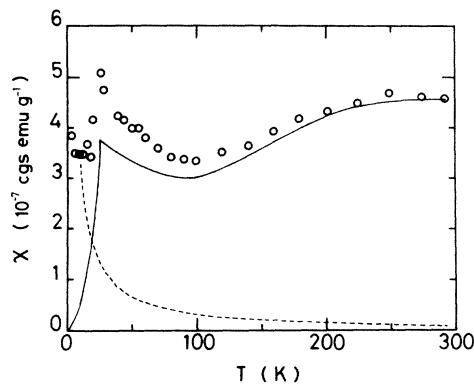


FIG. 3. Temperature dependence of the ESR intensity of the (2:1:0.5) phase for slow cooling. The solid line is obtained after the subtraction of the Curie tail at low temperatures. The Curie susceptibility is shown by the dashed line.

dependence above 20 K to that for rapid cooling. The concentration of localized spins is about the same as that for rapid cooling. (The concentration depends mainly on the quality of samples.)

Angular dependence of the  $g$  value and the linewidth  $\Delta H$  are shown for the (2:1:0.5) phase at 293 K in Fig. 4. The  $g$  value does not have temperature dependence. It has a maximum  $g_{\perp} = 2.0125$  for the applied field perpendicular to the  $a$ - $c$  plane, while it has a minimum  $g_{\parallel} = 2.0022$  for that parallel to the  $a$ - $c$  plane, which is almost around the  $g$  value of the free-electron spin ( $g_0 = 2.0023$ ).  $\Delta H$  has the similar angular dependence to the  $g$  value; the maximum and minimum linewidths are  $\Delta H_{\perp} = 33$  and  $\Delta H_{\parallel} = 23$  G for the applied field perpendicular and parallel to the  $a$ - $c$  plane, respectively. The linewidth is not affected by the conditions for a cooling process. Figure 5 shows the temperature dependence of the linewidth. The linewidth decreases linearly as the temperature is lowered, with a kink at around 110 K. The anisotropy in the linewidth becomes small as temperature decreases and, at

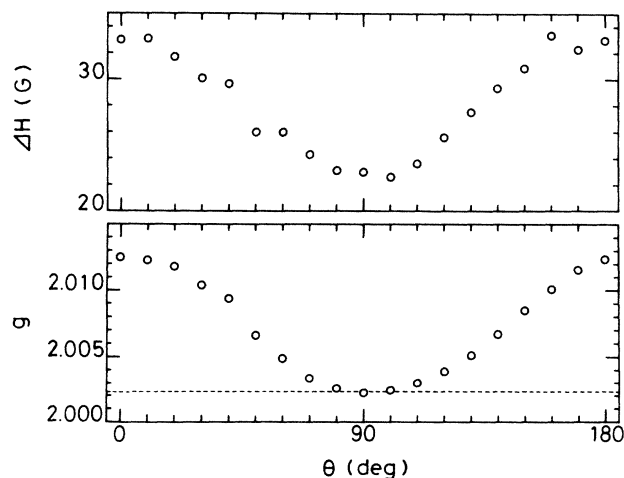


FIG. 4. Angular dependence of the  $g$  value and the linewidth  $\Delta H$  at 293 K for the (2:1:0.5) phase.  $\theta = 0^\circ$  and  $90^\circ$  correspond to the applied field directions perpendicular and parallel to the  $a$ - $c$  plane, respectively. The dashed line denotes the  $g$  value of free-electron spin.

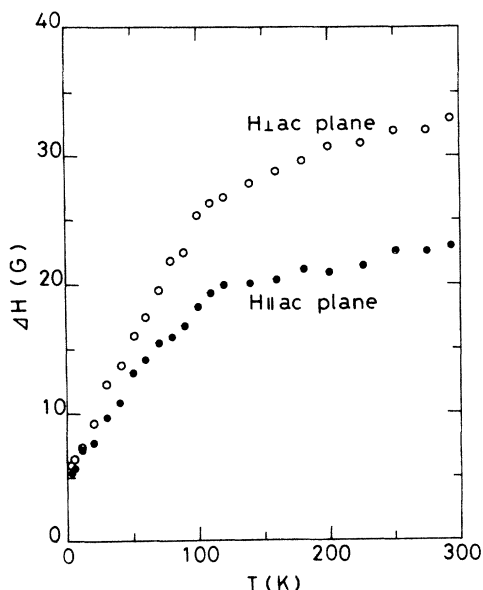


FIG. 5. Temperature dependence of the linewidth  $\Delta H$  for the (2:1:0.5) phase. The open circles denote the linewidth perpendicular to the  $a$ - $c$  plane, while the solid ones denote that parallel to the  $a$ - $c$  plane.

3 K, the linewidth, which is about 5 G, does not have an anisotropy. The line shape is Lorentzian in the observed temperature region.

Next, we show the results for the (3:2) phase. Figure 6 exhibits the temperature dependence of the ESR intensity. The intensity is almost constant in the high-temperature region down to 150 K. Below 150 K, it decreases exponentially as the lowering temperature and the Curie contribution becomes apparent below about 60 K. The estimated concentration of localized spins is about 0.4% of the BEDT-TTF molecules. The linewidth is anisotropic, which is  $\Delta H_c = 44$ ,  $\Delta H_{b'} = 53$ , or  $\Delta H_{a^*} = 65$  G at room temperature for the applied field parallel to the  $c$ ,  $b'$ , or  $a^*$  axes, respectively, where the  $b'$  axis is perpendicular to the  $c$  axis in the  $b$ - $c$  plane and the  $a^*$  axis is perpendicu-

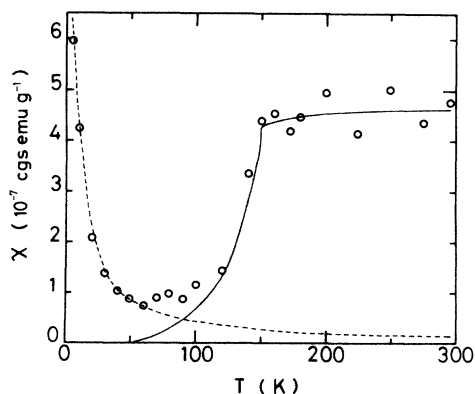


FIG. 6. Temperature dependence of the ESR intensity for the (3:2) phase. The solid line is obtained after the subtraction of the Curie tail at low temperatures. The Curie susceptibility is shown by the dashed line.

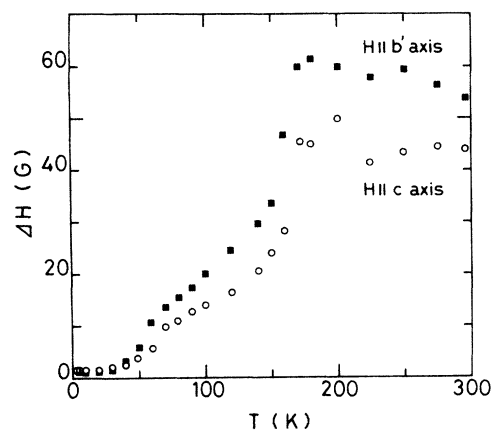


FIG. 7. Temperature dependence of the linewidth for the (3:2) phase. The solid squares denote the linewidth for the applied field parallel to the  $b'$  axis, while the open circles denote that for the applied field parallel to the  $c$  axis.

lar to the  $b$ - $c$  plane. The line shape is Lorentzian for the applied field parallel to the  $c$  and  $b'$  axes, while it is in between Lorentzian and Gaussian ones for the field parallel to the  $a^*$  axis. The temperature dependence of the linewidth is shown in Fig. 7. The linewidth increases gradually with decreasing temperature down to 170 K and decreases abruptly at 160 K. Then, it decreases monotonically until 70 K and begins to decrease more rapidly below 60 K. At 3 K, it becomes about 1 G with a small anisotropy.

Figure 8 shows the temperature dependence of the  $g$  values. The  $g$  values are independent of temperature in the high-temperature region down to about 200 K. Below the temperature,  $g_c$  decreases to a minimum around 160 K and increases until about 100 K. Below 100 K, it decreases gradually with decreasing temperature.  $g_{b'}$  increases steeply below about 200 K, whereas in the low-temperature region below about 120 K it becomes constant around 2.006.

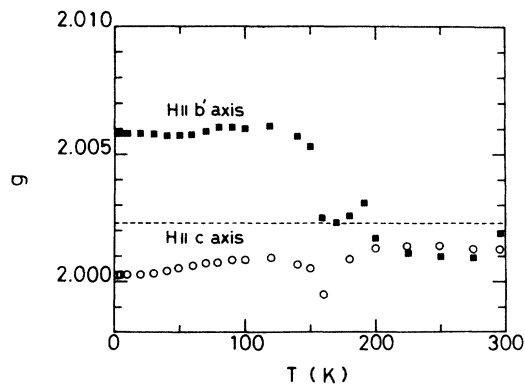


FIG. 8. Temperature dependence of the  $g$  value for the (3:2) phase. The solid squares denote the  $g$  value for the applied field parallel to the  $b'$  axis, while the open circles denote that for the applied field parallel to the  $c$  axis. The dashed line denotes the  $g$  value of free-electron spin.

### III. DISCUSSION

#### A. (BEDT-TTF)<sub>2</sub>ClO<sub>4</sub>(C<sub>2</sub>H<sub>3</sub>Cl<sub>3</sub>)<sub>0.5</sub>

In the (2:1:0.5)-phase crystal, the BEDT-TTF molecules are stacked along the [102] direction, while the biggest intermolecular overlapping is associated with the short side-by-side S-S contacts between the BEDT-TTF molecules along the  $[\bar{1}02]$  direction.<sup>17,18</sup> Thus, the cooperation of the face-to-face and the side-by-side intermolecular overlappings gives a two-dimensional conducting sheet in the  $a$ - $c$  plane, which is separated from the adjacent sheets by ClO<sub>4</sub><sup>-</sup> anions and C<sub>2</sub>H<sub>3</sub>Cl<sub>3</sub> solvent molecules. Since the long axis of the BEDT-TTF molecule is nearly parallel to the  $b^*$  axis, the axial direction of the  $p_\pi$  highest occupied molecular orbital of the BEDT-TTF molecule is perpendicular to the field direction when the field is applied parallel to the  $b^*$  axis. Therefore, the orientation of the BEDT-TTF molecule suggests a large  $g$  shift  $\delta g_b^* = (g_b^* - g_0)$  for the  $b^*$  axis which is in agreement with the experimental result as shown in Fig. 4. The positive  $g$  shift is attributable to the presence of hole carriers due to the BEDT-TTF donors. The resistivity shows metallic character down to 1.4 K for rapid cooling.<sup>6</sup> The magnetic susceptibility obtained from the ESR intensity can be explained with the Pauli paramagnetism. If we adopt a free-electron model, the magnetic susceptibility for the Pauli paramagnetism in a two-dimensional metal is given by

$$\chi_p = \frac{\mu_B^2 N}{\pi t}, \quad (1)$$

where  $t$  is the effective transfer integral in the two-dimensional sheet and  $N$  is Avogadro's number. From the above equation, we obtain the magnitude of the transfer integral  $t=0.05$  eV at room temperature. The estimation of the on-site Coulomb repulsion gives a still large  $U \sim 1.3$  eV for BEDT-TTF, taking into account  $U \sim 1.4$  eV for TTF (Refs. 19 and 20) and the difference in  $U$  between TTF and BEDT-TTF, 0.12 eV (Ref. 21), although the extended  $\pi$  system in the BEDT-TTF molecule, which is achieved through the chemical modification, reduces  $U$ . Therefore, the estimated  $t$  should be modified for the large on-site Coulomb repulsion. However, the small  $t$  is consistent with the theoretical results<sup>17,18</sup> and the optical reflectance experiment,<sup>22</sup> which suggest semimetallic character.

X-ray analysis<sup>23</sup> suggests thermal vibrations of the ClO<sub>4</sub><sup>-</sup> anions, the C<sub>2</sub>H<sub>3</sub>Cl<sub>3</sub> solvent molecules, and the ethylene groups  $-\text{CH}_2-\text{CH}_2-$  in the BEDT-TTF donor molecules, which reduce  $t$ , leading to the disturbance against the electron transport. The  $(2a \times b \times 2c)$  superlattice begins to develop gradually below about 200 K and is remarkable below about 150 K, which is associated with the antiparallel ordering of the C<sub>2</sub>H<sub>3</sub>Cl<sub>3</sub> solvent molecules with a dipole moment against thermal vibration.<sup>24</sup> Since the smallest distance between a Cl atom in the C<sub>2</sub>H<sub>3</sub>Cl<sub>3</sub> molecule and a C atom at an ethylene group in the BEDT-TTF molecule is about 2.7 Å,<sup>25</sup> it is suggested that the distance between an H atom in the BEDT-TTF molecule and a Cl atom in the C<sub>2</sub>H<sub>3</sub>Cl<sub>3</sub> molecule is smaller

than the van der Waals Cl-H distance ( $\sim 3$  Å), due to hydrogen bonding. Therefore, we can expect perceptible interactions between the ethylene group and the C<sub>2</sub>H<sub>3</sub>Cl<sub>3</sub> molecule, which will affect the vibration of the ethylene group. The ordering of the C<sub>2</sub>H<sub>3</sub>Cl<sub>3</sub> molecules induces suppression of the thermal vibration of the ethylene group, which may deviate the BEDT-TTF molecule from a planar structure, leading to the reduction of the intermolecular overlapping between adjacent BEDT-TTF molecules. The decrease in the susceptibility below about 200 K is explained with an enhancement in the magnitude of  $t$  through the reduction of the thermal vibration. The corrected susceptibility with a subtraction of the Curie-type susceptibility becomes nearly constant below about 100 K except at a temperature region approximately below the phase transition, observed at slow cooling, shown in Fig. 3. The magnitude of the susceptibility at 100 K gives  $t=0.06$  eV, which is larger by 20% than that at room temperature.

For a slow-cooling run, a metal-insulator transition takes place at 20 K as shown in Fig. 3. Since the (2:1:0.5)-phase crystal has a  $\frac{3}{4}$ -filled band, the metal-insulator transition is considered to be a nesting transition to an insulating state with a fourfold superlattice, which is associated with the ordering of the solvent C<sub>2</sub>H<sub>3</sub>Cl<sub>3</sub> molecules. The transition temperature is quite low in comparison with that of a similar compound, (TMTTF)<sub>2</sub>ClO<sub>4</sub> ( $T_c=75$  K).<sup>5</sup> The (2:1:0.5)-phase crystal is a two-dimensional metal with a cooperation of the side-by-side and the face-to-face interactions, where the ratio of the transfer integrals is estimated to be  $t_\perp/t_\parallel \sim 1$ .<sup>17,18</sup> The two-dimensionality depresses the transition temperature for the nesting transition. For a rapid-cooling run, the nesting transition disappears, even though the resistivity shows a small increase below about 20 K.<sup>6</sup> The correlation lengths for the establishment of the  $(2a \times b \times 2c)$  superstructure are quite small even at low temperatures around 20 K (i.e.,  $\xi_a=13$  Å,  $\xi_b=25$  Å, and  $\xi_c=55$  Å at 125 K), due to some intrinsic disorder remaining in the host lattice.<sup>24</sup> The Curie tail of the susceptibility suggests the presence of localized spins attributed to lattice irregularities which might lead to a finite-chain behavior. Our result indicates that the concentration of the chain-interrupting species with localized spins is 0.1–0.3% of the number of the BEDT-TTF molecules. This means the existence of one chain-interrupting specie per 7–10 BEDT-TTF molecules in a donor chain is comparable to the correlation range of the  $(2a \times b \times 2c)$  superlattice ( $\xi_a/a \sim 1$ ,  $\xi_b/b \sim 1.3$ , and  $\xi_c/c \sim 7$ ). The presence of the intrinsic disorder in the host lattice gives an incomplete ordering of the C<sub>2</sub>H<sub>3</sub>Cl<sub>3</sub> solvent molecules depending on both the quality of samples and the cooling rate of the sample. The intrinsic disorder will easily cause a considerable degree of incompleteness in the ordering of the C<sub>2</sub>H<sub>3</sub>Cl<sub>3</sub> solvent molecules for rapid cooling. The random potentials generated by the incomplete ordering will obscure the Fermi surface, leading to the suppression of the nesting transition if the magnitude of randomness in the potential ( $\Delta V$ ) overwhelms the gap ( $\Delta$ ) generated by the transition. Therefore, the disappearance of the transition for rapid cooling can be explained with the large random-

ness  $\Delta V > \Delta$ .

Next, we discuss the linewidth depending on temperature. The linewidth is described by the contributions from spin-lattice relaxation ( $T_1$ ) and spin-spin relaxation ( $T_2$ ). In the case of the (2:1:0.5)-phase crystal, the contribution from  $T_2$ , which is associated with dipole-dipole interactions, is negligible due to motional narrowing, taking into account the Lorentzian line shape. For metallic systems, the spin-lattice relaxation is understood by means of the Elliott mechanism,<sup>26</sup> where the energy of a spin system flows to a lattice system through a spin flip by the spin-orbit interaction and a scattering of conduction electrons by acoustic phonons. Since the relaxation by the Elliott mechanism is forbidden in a pure one-dimensional conducting system, the linewidth is quite narrow [ $\Delta H = 2.5\text{--}5$  G for  $(\text{TMTTF})_2X$  ( $X = \text{PF}_6^-$ ,  $\text{ClO}_4^-$ , and  $\text{Br}^-$ )<sup>5</sup>]. The large linewidth ( $\Delta H_{\perp} = 33$  G and  $\Delta H_{\parallel} = 23$  G) of the (2:1:0.5) phase suggests two-dimensionality, where the relaxation is allowed through the interchain hoppings. This is consistent not only with the small anisotropy in the resistivity,<sup>6</sup> but also with the band calculation.<sup>17,18</sup> The linewidth  $\Delta H$  is related to conductivity  $\sigma$  in the equations  $\Delta H = T_1^{-1} \sim (\delta g)^2/\tau$  and  $\sigma = ne^2\tau/m$ , where  $\tau$  is a relaxation time for the conduction. Since the conductivity increases with lowering temperature, the temperature dependence of the linewidth is qualitatively in agreement with the Elliott mechanism.

#### B. $(\text{BEDT-TTF})_3(\text{ClO}_4)_2$

The BEDT-TTF molecules are stacked along the  $[0\bar{1}1]$  direction in the  $b$ - $c$  plane, while the biggest intermolecular overlapping is associated with the short side-by-side S-S contacts between the BEDT-TTF molecules along the  $[012]$  direction.<sup>9</sup> The side-by-side intermolecular overlapping gives a quasi-one-dimensional conducting chain along the  $[012]$  direction. The two-dimensional network of the BEDT-TTF molecules composed of the larger side-by-side and the smaller face-to-face overlapping in the  $b$ - $c$  plane is separated from the adjacent ones by  $\text{ClO}_4^-$  anions. The long axis of the BEDT-TTF molecule is nearly parallel to the  $a^*$  axis.

The temperature dependence of resistivity shows a metal-insulator transition at 174 K with an activation energy  $E_a = 0.26$  eV. The susceptibility for the Pauli paramagnetism in a one-dimensional metal is related to the transfer integral  $t_{\parallel}$  parallel to the one-dimensional chain by means of the tight-binding model by

$$\chi_p = \frac{\mu_B^2 N}{\pi \sin(\pi N'/2)} \frac{1}{t_{\parallel}}, \quad (2)$$

where  $N'$  is the amount of charge transfer per donor molecule.  $\chi_p$  at  $T > T_c$  ( $= 150$  K for the ESR measurement) gives the transfer integral  $t_{\parallel} = 0.06$  eV, using Eq. (2) with  $N' = \frac{2}{3}$ . The small  $t_{\parallel}$  is consistent with the results of the band calculation,<sup>9</sup> though the estimation must be corrected for  $U \sim 1.3$  eV. Below  $T_c$ , an exponential decrease in the susceptibility suggests a singlet ground state. The change in the  $g$  value  $g_b$  and  $g_c$  at  $T_c$  with a precursor in the rather wide critical region ( $T_c < T < \sim 200$  K), as shown in Fig. 8, is considered to be associated with the

displacement of the BEDT-TTF molecules in a one-dimensional chain. Since the (3:2) phase has a  $\frac{2}{3}$ -filled band,  $2k_F$  and  $4k_F$  lattice distortions are equivalent. The considerably large on-site Coulomb repulsion  $U$  prefers the  $4k_F$  distortion with threefold periodicity. At room temperature, x-ray analysis shows that the (3:2) phase has the threefold periodicity of the BEDT-TTF molecules.<sup>9</sup> Taking into account the metallic properties revealed by the susceptibility and resistivity, the energy gap due to the periodicity is thought to be smaller than thermal energy at  $T > T_c$ . The metal-insulator transition may be explained as a transition of the Peierls instability with the  $4k_F$  distortion, which is similar to that of  $(\text{BEDT-TTF})_3(\text{ReO}_4)_2$ .<sup>27</sup>

The (3:2) phase has a large linewidth at room temperature;  $\Delta H_{a^*} = 65$ ,  $\Delta H_{b^*} = 53$ , and  $\Delta H_{c^*} = 44$  G. The line shape for the applied field parallel to the  $a^*$  axis is in between a Gaussian and a Lorentzian shape. This means an incomplete motional narrowing against the dipolar field is due to the restricted spin diffusion in the low-dimensional system,<sup>28</sup> since the interchain hopping rate is very small for the direction parallel to the  $a^*$  axis, as expected through the crystal structure and the anisotropy in the resistivity  $\rho[\text{parallel to the } (100) \text{ plane}]/\rho[\text{normal to the } (100) \text{ plane}] = 10^{-4}$ .<sup>9</sup> The large linewidth  $\Delta H_{b^*}$  and  $\Delta H_{c^*}$  can be considered to be associated with the spin-phonon mechanism allowed through the two-dimensionality, taking into account the Lorentzian line shapes. The linewidth  $\Delta H$  is given by<sup>29</sup>

$$T_1^{-1} \sim \frac{(\delta g)^2}{g} \frac{\hbar \Delta E^2}{\mu_B t_{\parallel}^2 \tau_{\perp}}, \quad (3)$$

where  $\tau_{\perp}$  is the scattering time perpendicular to the conducting chain in the  $b$ - $c$  plane and  $\Delta E$  is a typical molecular orbital energy difference. The interchain hopping rate in the  $b$ - $c$  plane is estimated to be  $\tau_{\perp} \sim 10^{-13}$  sec from Eq. (3), if we take  $\Delta E \sim 4t_{\parallel}$ . This is consistent with the band calculation which shows a quasi-one-dimensionality in the transfer integrals.<sup>9</sup>

#### IV. SUMMARY

The magnetic properties of two  $(\text{BEDT-TTF})\text{-ClO}_4$  radical salts,  $(\text{BEDT-TTF})_2\text{ClO}_4(\text{C}_2\text{H}_3\text{Cl}_3)_{0.5}$  and  $(\text{BEDT-TTF})_3(\text{ClO}_4)_2$ , have been investigated by means of ESR measurement. In the case of the (2:1:0.5) phase, the magnetic susceptibility shows the Pauli paramagnetism down to a nesting transition of 20 K for slow cooling of the sample. The suppression of the thermal vibrations of the ethylene groups in the BEDT-TTF donors by the interactions between the ethylene group and the  $\text{C}_2\text{H}_3\text{Cl}_3$  solvent molecule enhances the transfer integral  $t$  in a two-dimensional BEDT-TTF conducting sheet at low temperatures below about 200 K, as the  $\text{C}_2\text{H}_3\text{Cl}_3$  molecules begin to be ordered to form the  $(2a \times b \times 2c)$  superlattice below the temperature. For rapid cooling, the metallic properties persist even below  $T_c$ , consistent with the result of the resistivity measurement.<sup>6</sup> The random potentials, which are generated by the incomplete ordering of the  $\text{C}_2\text{H}_3\text{Cl}_3$  molecules at low temperatures associated with intrinsic disorder in the host lattice, obscure the Fermi

surface to suppress the nesting transition. The large linewidth suggests the two dimensionality of the conducting system, consistent with the low  $T_c$  for the transition.

The (3:2)-phase crystal has a metal-insulator transition at  $T_c = 150$  K. Below  $T_c$ , an insulating state with a spin singlet is stabilized after the displacement of the BEDT-TTF donor molecules in a one-dimensional chain through the Peierls instability, judging from the exponential decrease in the susceptibility and the change in the  $g$  values. An incomplete motional narrowing for the direction parallel to the  $a^*$  axis is consistent with the very small interchain hopping rate in this direction expected with the

large anisotropy in the resistivity  $\rho_{\parallel}/\rho_{\perp} = 10^{-4}$ . The large linewidth  $\Delta H_b$  and  $\Delta H_c$  suggests the large interchain hopping rate in the  $b$ - $c$  plane.

#### ACKNOWLEDGMENTS

The authors wish to thank Dr. H. Ohya of Kyoto University, and Professor K. Nasu and Dr. T. Mori of the Institute for Molecular Science for their helpful discussions. They also express their gratitude to Professor H. Kobayashi of Toho University for his kind offer of the x-ray results.

- <sup>1</sup>D. Jerome and H. J. Schulz, *Adv. Phys.* **31**, 299 (1982). [TMTSF is an abbreviation for 2,3,6,7-tetramethyl-1,4,5,8-tetraselenafulvalene, with the chemical formula  $(\text{CH}_3)_4\text{C}_6\text{Se}_4$ .]
- <sup>2</sup>F. Wudl and E. Aharon-Schalom, *J. Am. Chem. Soc.* **104**, 1154 (1982).
- <sup>3</sup>G. Saito, T. Enoki, H. Inokuchi, H. Kumagai, and J. Tanaka, *Chem. Lett.* **1983**, 503.
- <sup>4</sup>P. Delhaes, C. Coulon, J. Amiel, S. Flandrois, E. Toreilles, J. M. Fabre, and L. Giral, *Mol. Cryst. Liq. Cryst.* **50**, 43 (1979). [TMTTF is an abbreviation for 2,3,6,7-tetramethyl-1,4,5,8-tetrathiafulvalene, with the chemical formula  $(\text{CH}_3)_4\text{C}_6\text{S}_4$ .]
- <sup>5</sup>C. Coulon, P. Delhaes, S. Flandrois, R. Lagnier, E. Benjour, and J. M. Fabre, *J. Phys. (Paris)* **43**, 1059 (1982).
- <sup>6</sup>G. Saito, T. Enoki, K. Toriumi, and H. Inokuchi, *Solid State Commun.* **42**, 557 (1982).
- <sup>7</sup>H. Kobayashi, T. Mori, R. Kato, A. Kobayashi, Y. Sasaki, G. Saito, and H. Inokuchi, *Chem. Lett.* **1983**, 581.
- <sup>8</sup>H. Kobayashi, R. Kato, T. Mori, A. Kobayashi, Y. Sasaki, G. Saito, and H. Inokuchi, *Chem. Lett.* **1983**, 759.
- <sup>9</sup>H. Kobayashi, R. Kato, T. Mori, A. Kobayashi, Y. Sasaki, G. Saito, T. Enoki, and H. Inokuchi, *Chem. Lett.* **1984**, 179.
- <sup>10</sup>H. Kobayashi, A. Kobayashi, Y. Sasaki, G. Saito, and H. Inokuchi, *Chem. Lett.* **1984**, 183.
- <sup>11</sup>S. S. P. Parkin, E. M. Engler, R. R. Schumaker, R. Lagier, V. Y. Lee, J. C. Scott, and R. L. Greene, *Phys. Rev. Lett.* **50**, 270 (1983).
- <sup>12</sup>E. B. Yagubskii, I. F. Shchegolev, V. N. Laukhin, P. A. Kononovich, M. V. Karatsovnik, A. V. Zvarykina, and L. I. Buravov, *Pis'ma Zh. Eksp. Teor. Fiz.* **39**, 12 (1984) [*JETP Lett.* **39**, 12 (1984)].
- <sup>13</sup>G. W. Crabtree, K. D. Carlson, L. N. Hall, P. T. Copps, H. H. Wang, T. J. Emge, M. A. Beno, and J. M. Williams, *Phys. Rev. B* **30**, 2958 (1984).
- <sup>14</sup>K. Murata, M. Tokumoto, H. Anzai, H. Bando, G. Saito, K. Kajimura, and T. Ishiguro, *J. Phys. Soc. Jpn.* **54**, 1236 (1985).
- <sup>15</sup>E. B. Yagubskii, I. F. Shchegolev, V. N. Topnikov, S. I. Pesotskii, V. N. Laukhin, P. A. Kononovich, M. V. Kartsovnik, A. V. Zvarykina, S. G. Dedik, and L. I. Buravov, *Zh. Eksp. Teor. Fiz.* **88**, 244 (1985) [*Sov. Phys.—JETP* **61**, 142 (1985)].
- <sup>16</sup>W. Duffy, Jr., *J. Chem. Phys.* **36**, 490 (1962).
- <sup>17</sup>T. Mori, A. Kobayashi, Y. Sasaki, H. Kobayashi, G. Saito, and H. Inokuchi, *Chem. Lett.* **1982**, 1963.
- <sup>18</sup>T. Mori, A. Kobayashi, Y. Sasaki, H. Kobayashi, G. Saito, and H. Inokuchi, *Bull. Chem. Soc. Jpn.* **57**, 627 (1984).
- <sup>19</sup>J. B. Torrance, B. A. Scott, B. Welber, F. B. Kaufman, and P. E. Seiden, *Phys. Rev. B* **19**, 730 (1979).
- <sup>20</sup>Y. Cao, K. Yakushi, and H. Kuroda, *Solid State Commun.* **35**, 601 (1980).
- <sup>21</sup>G. Saito, T. Enoki, M. Kobayashi, K. Imaeda, N. Sato, and H. Inokuchi, *Mol. Cryst. Liq. Cryst.* **119**, 393 (1985).
- <sup>22</sup>H. Tajima, K. Yakushi, H. Kuroda, G. Saito, and H. Inokuchi, *Solid State Commun.* **49**, 769 (1984).
- <sup>23</sup>H. Kobayashi, A. Kobayashi, Y. Sasaki, G. Saito, T. Enoki, and H. Inokuchi, *J. Am. Chem. Soc.* **105**, 297 (1983).
- <sup>24</sup>S. Kagoshima, J. P. Pouget, G. Saito, and H. Inokuchi, *Solid State Commun.* **45**, 1001 (1983).
- <sup>25</sup>H. Kobayashi (private communications).
- <sup>26</sup>R. J. Elliott, *Phys. Rev.* **96**, 266 (1954).
- <sup>27</sup>K. Carneiro, J. C. Scott, and E. M. Engler, *Solid State Commun.* **50**, 477 (1984).
- <sup>28</sup>P. M. Richards, *Magnetic Resonance in One- and Two-Dimensional Systems, Enrico Fermi Proceedings of the International School of Physics, Course 59* (North-Holland, Amsterdam, 1976).
- <sup>29</sup>H. J. Pederson, J. C. Scott, and K. Bechgaard, *Phys. Rev. B* **24**, 5014 (1981).